


Spreading depolarization causes reperfusion failure after cerebral ischemia

Journal of Cerebral Blood Flow & Metabolism
0(0) 1–10
© The Author(s) 2023
Article reuse guidelines:
sagepub.com/journals-permissions
DOI: 10.1177/0271678X231153745
journals.sagepub.com/home/jcbfm



Anna Törteli^{1,2}, Réka Tóth^{1,2}, Sarah Berger²,
Sarah Samardzic², Ferenc Bari³, Ákos Menyhárt^{1,2} and
Eszter Farkas^{1,2} 

Abstract

Despite successful recanalization, reperfusion failure associated with poor neurological outcomes develops in half of treated stroke patients. We explore here whether spreading depolarization (SD) is a predictor of reperfusion failure. Global forebrain ischemia/reperfusion was induced in male and female C57BL/6 mice ($n = 57$). SD and cerebral blood flow (CBF) changes were visualized with transcranial intrinsic optical signal and laser speckle contrast imaging. To block SD, MK801 was applied ($n = 26$). Neurological deficit, circle of Willis (CoW) anatomy and neuronal injury were evaluated 24 hours later. SD emerged after ischemia onset in one or both hemispheres under a perfusion threshold (CBF drop to 21.1 ± 4.6 vs. $33.6 \pm 4.4\%$, SD vs. no SD). The failure of later reperfusion ($44.4 \pm 12.5\%$) was invariably linked to previous SD. In contrast, reperfusion was adequate ($98.9 \pm 7.4\%$) in hemispheres devoid of SD. Absence of the PI segment of the posterior cerebral artery in the CoW favored SD occurrence and reperfusion failure. SD occurrence and reperfusion failure were associated with poor neurologic function, and neuronal necrosis 24 hours after ischemia. The inhibition of SD significantly improved reperfusion. SD occurrence during ischemia impairs later reperfusion, prognosticating poor neurological outcomes. The increased likelihood of SD occurrence is predicted by inadequate collaterals.

Keywords

Circle of Willis, collaterals, ischemic stroke, reperfusion, spreading depolarization

Received 9 September 2022; Revised 2 December 2022; Accepted 3 January 2023

Introduction

Recanalization is the only therapeutic choice to treat acute ischemic stroke and is one of the strongest predictors of favorable outcome and reduced mortality rate.¹ However, in almost half of the patients, recanalization is futile, and there is no neurological improvement despite optimal angiographic results.^{2,3} Futile recanalization or reperfusion failure is associated with older age and poor collaterals.^{1,2} Despite frequent diagnosis, the mechanistic background of reperfusion failure has remained unresolved. The pathomechanisms suspected to account for reperfusion failure include microvascular no-reflow due to embolization, neutrophil obstruction or pericyte constriction, next to large vessel constriction.⁴ In our present work, we explore the possibility that ischemic spreading depolarization

¹Hungarian Centre of Excellence for Molecular Medicine – University of Szeged, Cerebral Blood Flow and Metabolism Research Group, Szeged, Hungary

²Department of Cell Biology and Molecular Medicine, Albert Szent-Györgyi Medical School and Faculty of Science and Informatics, University of Szeged, Szeged, Hungary

³Department of Medical Physics and Informatics, Albert Szent-Györgyi Medical School and Faculty of Science and Informatics, University of Szeged, Szeged, Hungary

Corresponding authors:

Ákos Menyhárt, Hungarian Centre of Excellence for Molecular Medicine – University of Szeged, Cerebral Blood Flow and Metabolism Research Group, Szeged, Hungary.
Email: menyhart.akos@med.u-szeged.hu

Eszter Farkas, Department of Cell Biology and Molecular Medicine, Albert Szent-Györgyi Medical School and Faculty of Science and Informatics, University of Szeged, Szeged, Hungary.
Email: eszter.farkas@hccmm.eu

(SD), a potent pathophysiological phenomenon is a reliable predictor of reperfusion failure.

SD develops in a recurrent pattern in the ischemic cortex of malignant hemispheric stroke patients as recorded during decompressive hemicraniectomy⁵ or over the first week after the surgical procedure.^{6–8} SD occurs first within minutes after the onset of vascular occlusion.⁹ SD represents the abrupt near-complete breakdown of the transmembrane ion gradients in a critical volume of gray matter, which propagates as a wave over the nervous tissue.¹⁰ The pathophysiological relevance of SD is thought to lie in the formation of cytotoxic edema, the accumulation of glutamate, and the building up of a massive acid load in the wake of the wavefront, which initiate intracellular cell death cascades.^{11–13} Most importantly, massive increases in intracellular sodium and calcium concentrations occur with the SD wavefront.^{10,14,15} In the acutely injured human cortex, specific SD patterns have been associated with lesion maturation and the development of delayed infarctions.^{16–18} These reports and accumulating experimental evidence collectively testify that SDs spontaneously evolve during acute brain injury, initiate primary ischemic lesions and facilitate infarct growth.¹⁹ However, any putative relationship between SD and reperfusion failure has remained unattended.

Here we set out to demonstrate in the mouse cortex that SD that occurs during an ischemic episode has a profound impact on the success of subsequent reperfusion.

Materials and methods

Animals

The experimental procedures were approved by the National Food Chain Safety and Animal Health Directorate of Csongrád-Csanád County, Hungary. The procedures were performed according to the guidelines of the Scientific Committee of Animal Experimentation of the Hungarian Academy of Sciences [updated Law and Regulations on Animal Protection: 40/2013. (II. 14.) Gov. of Hungary], following the EU Directive 2010/63/EU on the protection of animals used for scientific purposes, and reported in compliance with the ARRIVE guidelines. The mice – obtained from the Charles River colony at the Biological Research Centre, Centre of Excellence of the European Union, Szeged, Hungary – were group-housed and kept under normal 12-h light/dark cycle, with *ad libitum* access to food and tap water.

Surgical procedures

Young adult (10–12 weeks old) male ($n=28$) and female ($n=29$) C57BL/6 mice ($m=25–31$ g) were

anesthetized with isoflurane (0.6–0.9% in $N_2O:O_2$) and allowed to breath spontaneously through a nose cone. Body temperature was maintained at 37°C using a thermostat-controlled heating pad (CODA monitor, Kent Scientific Corp., Torrington, CT, USA). Topical Lidocaine (1%) was administered at incisions. The common carotid arteries (CCAs) were separated, and silk threads were looped around the arteries for later occlusion. Mice were then fixed in the prone position in a stereotactic frame. A midline incision was made above the sagittal suture, and the skin was gently pulled aside. The entire skull surface was covered with UV light adhesive (UV683 Light Curing Adhesive, Permabond Ltd., Wessex, UK) to increase transparency and to avoid drying out.

Intrinsic optical signal (IOS) imaging and laser speckle contrast analysis (LASCA) through the intact skull

SD propagation was tracked by IOS imaging, while cerebral blood flow (CBF) changes were monitored with LASCA.²⁰ The entire cortical surface (both hemispheres) was illuminated in a stroboscopic mode with a light emitting diode (LED) (530 nm peak wavelength; SLS-0304-A, Mightex Systems, Pleasanton, CA, USA) and a laser diode (HL6545MG, Thorlabs Inc., New Jersey, USA; 120 mW; 660 nm emission wavelength) driven by a power supply (LDTC0520, Wavelength Electronics, Inc., Bozeman, USA) set to deliver a 160-mA current. Both image sequences were captured with a monochrome CCD camera (resolution: 1024 × 1024 pixel, Pantera 1M30, DALSA, Gröbenzell, Germany) attached to a stereomicroscope (MZ12.5, Leica Microsystems, Wetzlar, Germany). LED (100 ms/s) and laser illuminations (2 ms/s) and camera exposure times (100 ms/s for both LED and laser) were synchronized by a dedicated program written in LabVIEW. Background images were captured by the same camera at a 1 frame/s rate to be used for offline correction of raw images.

Experimental protocol and post-operative care

Multi-modal optical imaging of the mouse brain surface started with a baseline period of 10 min, followed by the bilateral occlusion of the CCAs (2-vessel occlusion; 2VO) for 45 minutes to induce incomplete global forebrain ischemia. The CCAs were then released to allow reperfusion, which was monitored for an additional 75 minutes. The wounds were sutured, and the animals were transferred to an incubator cage (32°C) for 2 hours and allowed to wake up. Wounds were treated with Betadine (10 mg/ml, Egis) and Lidocaine

(10 mg/ml, Egis) for local analgesia. Animals were hydrated by the administration of warmed (37°C) saline (2 ml) subcutaneously. For long term analgesia, mice received a subcutaneous injection of the non-steroid anti-inflammatory drug Carprofen (5 mg/kg; Rycarfa, 8501 Novo Mesto, Slovenia). Finally, animals were supplied with fresh water and a softened standard chow in a recovery cage for 24 hours.

Pharmacologic SD blockade

To attenuate SD evolution, the non-competitive NMDA receptor antagonist MK801 (Sigma-Aldrich, St. Louis, MO, USA) was administered in a separate cohort (0.3 mg/kg, i.p., $n=26$), 30 min prior to ischemia induction.

Invasive mean arterial blood pressure (MABP) measurements

In additional mice (Control: $n=5$, MK801: $n=7$), MABP was measured invasively over the experimental protocol through a catheter inserted into the left femoral artery. The MABP signal was digitized in a dedicated hardware and software environment (Biopac MP150 and Acknowledge 4.2, Biopac Systems Inc., USA). Systemic blood gas analysis was performed 20 minutes before recording. Physiological variables (MABP, arterial partial pressure of O_2 , CO_2 and pH) were in the physiological range (Table S1-S2).

Characterization of post-stroke neurological deficit

Neurological score was taken a day before (baseline) and 24 hours after stroke (Figure 1). Sensorimotor function was evaluated with the Composite Garcia Neuroscore (GN) scale.²¹ The total score for the GN test ranges from 0 (severe impairment) to 21 (no deficit). All test domains were performed in the same order for each animal.

Evaluation of the circle of Willis (CoW) anatomy

Mice were transcardially perfused under deep anaesthesia with saline and 4% paraformaldehyde (PFA), followed by carbon black ink. The brains were carefully removed, and the CoW was evaluated with a stereomicroscope (Alpha STO-4M, Elektro-Optika Kft., Hungary) equipped with a Nikon-DS Fi3 camera.

Hematoxylin-eosin staining to assess cell damage

After the anatomical evaluation of the CoW, 10 control and 10 MK801-treated brains were cut to 10- μ m thick frozen sections with a freezing microtome (Leica CM

1860 UV, Leica, Germany). The sections were stained with hematoxylin and eosin (Sigma-Aldrich, USA) and cover slipped with Eukit[®] (Merck, USA). Photomicrographs of the sections were taken at 40 \times magnification with a Nikon-DS Fi3 camera attached to a Leica DM 2000 Led light microscope (Leica Microsystems GmbH, Germany).

Data analysis and statistics

Power analysis for pharmacological experiments followed established principles. The pilot experiments indicated differences between the experimental groups (MK801 vs. Control) and achieved the confidence level of 95% and a power of 80% at low sample size ($\alpha=0.05$ and β (type II error) of 0.2). As calculated, sufficient statistical power was assumed at a final sample size of 11–12 animals/group. The calculations were run in GPower 3.1 (Heinrich Heine University of Düsseldorf, Germany).

All mice were coded independent of treatment or sex and randomly allocated to experimental groups. The four investigators performing surgeries, neuroscoring, reperfusion efficacy and infarct size calculation were completely blinded to treatment and animal gender. Six animals were excluded because ischemic injury was lethal during recording ($n=2$) or overnight to Day 1 ($n=4$).

Raw image sequences were analyzed in ImageJ (National Institute of Health, Bethesda, USA) and AcqKnowledge 4.2.0 (Biopac Systems Inc., USA). Local changes in IOS intensity and CBF with time were extracted by placing regions of interest (ROIs; 50 \times 50 pixels, 0.4 \times 0.4 mm) at selected sites in the images. CBF recordings obtained by LASCA were expressed relative to baseline by using the average CBF of the first 5 minutes of baseline (100%) and the recorded biological zero after terminating each experiment (0%). Neuronal necrosis was evaluated using the inbuilt automatized Plug-in “analyze particles” in ImageJ. Data are given as mean \pm stdev. Each data set was first evaluated with a Shapiro-Wilk test of normality to guide the choice of parametric or non-parametric statistics. Statistical analysis was conducted with the software SigmaPlot 12.5 (Systat Software, Inc., San Jose, CA, USA). Distinct statistical methods are provided in detail in each Figure legend.

AT and ÁM have full access to all the data in the study and takes responsibility for its integrity and the data analysis. Raw data are available from the Authors upon reasonable request.

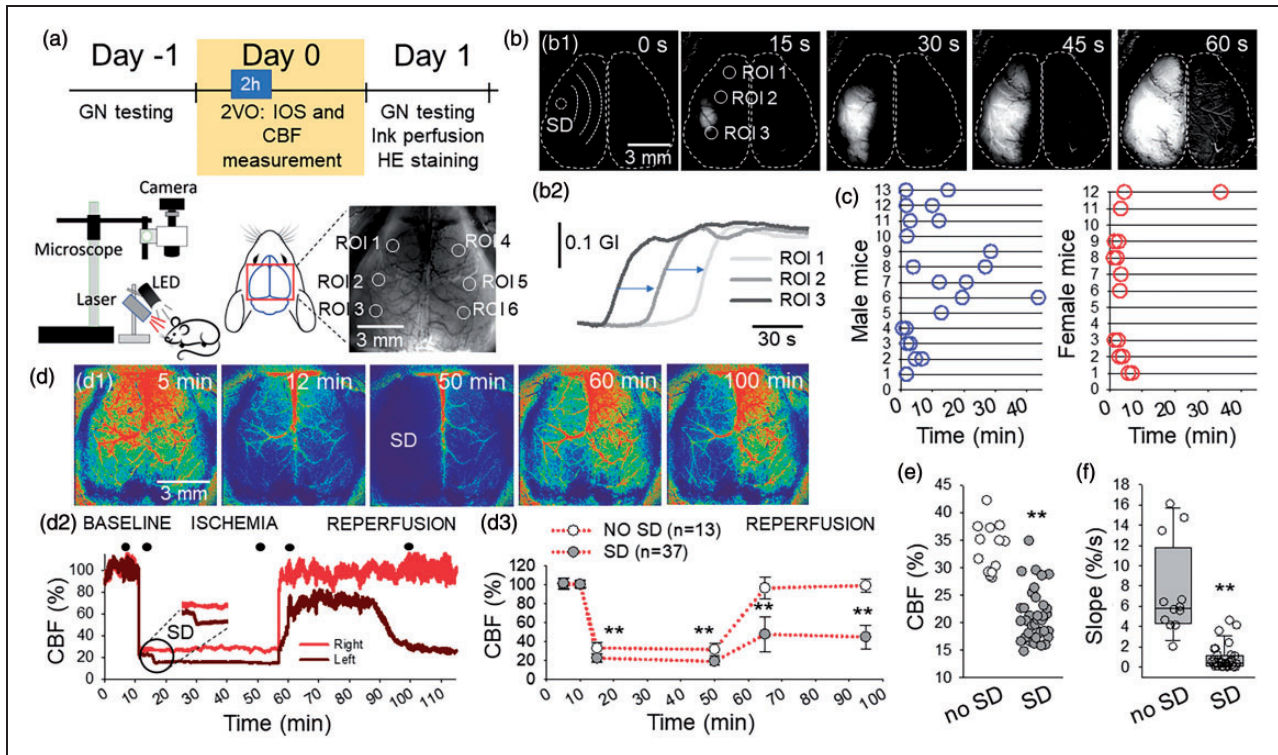


Figure 1. IOS and CBF imaging reveals spatial coincidence between the occurrence of SD during ischemia and the subsequent insufficiency of reperfusion. (a) The timeline of the experiments, the arrangement of the imaging setup, and a representative raw transcranial IOS image of the mouse cortex with regions of interest placed offline (ROIs 1–6). (b) A representative IOS image sequence of the cortical surface after background subtraction (b₁) and corresponding IOS intensity traces (b₂) demonstrate the unilateral occurrence of SD. (c) The temporal pattern of first SD per hemisphere over the ischemic period (45 min) in male (n = 13) and female (n = 12) mice. (d) Representative CBF maps (d₁) of the same preparation as in b, and corresponding CBF traces (at ROI2 and ROI5 in a) (d₂) show the spatial coincidence between SD occurrence and reperfusion failure. CBF images correspond in time with the closed circles over the CBF traces. Mean CBF values (d₃) show significant reperfusion failure ipsilateral to ischemic SD at 15 and 45 min after the release of the carotid arteries. Note complete reperfusion in the hemisphere devoid of SD under ischemia. (e) SD occurrence was linked to a greater drop of CBF after ischemia onset and (f) Reperfusion ipsilateral to SD developed at a considerably slow rate (slope). Data are given as individual values (c & e), mean \pm stdev (d₃) or in a box plot (f). The distribution of data was evaluated with a Shapiro-Wilk test (d₂: $p = 0.065$, e: $p < 0.050$, f: $p < 0.050$), followed by a One-Way RM ANOVA with Holm-Sidak post-hoc test (d₃) and a Mann-Whitney Rank Sum Test (e&f), $p < 0.01^{**}$.

Results

Spatial coincidence between SD during ischemia and subsequent reperfusion failure

Transcranial IOS imaging revealed the occurrence and propagation of SD over the mouse cerebral cortex during ischemia (Figure 1(a) and (b)). Three distinct SD patterns were observed: (i) SD evolved in each hemisphere (bilateral SD, $n = 9/6$, male/female; the two SDs emerged at unrelated foci in the two hemispheres and were apart in time), (ii) SDs predominantly occurred in one hemisphere (unilateral SD, $n = 4/3$, male/female), or (iii) SD was not seen in either of the hemispheres (no SD, $n = 0/3$, male/female). Altogether, 37 SDs were recorded in 25 mice. SD occurrence was slightly more likely in males than in females

(hemispheres implicated in SD evolution: $n = 22/15$, male/female).

CBF imaging indicated a sharp drop of CBF upon ischemia onset (Figure 1(d)). A greater reduction of perfusion favored SD evolution (CBF drop to 21.1 ± 4.6 vs. $33.6 \pm 4.4\%$, SD vs. no SD) (Figure 1(e)). In case SD occurred, a further flow reduction known as spreading ischemia was coupled to SD (to 18.6 ± 4.3 vs. $31.2 \pm 6.3\%$, SD vs. no SD) (Figure 1(d)). Upon the release of the CCAs, reperfusion failure was seen in the hemisphere that had been engaged in SD (47.2 ± 18.3 and $44.4 \pm 12.5\%$, 15 min and 45 min after reperfusion initiation). In contrast, perfusion recovered to pre-ischemic levels in case the hemisphere had not undergone SD (96.3 ± 11.9 and $98.9 \pm 7.4\%$, 15 min and 45 min after reperfusion initiation) (Figure 1(d)). Reperfusion failure after SD was also reflected by the

low rate of flow elevation after the release of the carotid arteries, in contrast with the sharp rise of CBF in the hemisphere devoid of prior SD (0.87 ± 1.19 vs. $7.45 \pm 4.60\%/s$, SD vs. no SD) (Figure 1(f)).

The link between incomplete CoW and greater CBF reduction favoring SD

The CoW is often incomplete in young adult C57BL/6 mice.²² The P1 segment of the posterior cerebral artery (PCA) is frequently absent or dysplastic.²³ Accordingly, the absence of the P1 segment in our mouse cohort was observed regularly (Figure 2). Importantly, the absence of P1 predicted greater perfusion drop in the ipsilateral hemisphere (to 21.3 ± 5.0 vs. $30.8 \pm 6.3\%$, P1 absent vs. P1 present), which

generally coincided with the occurrence of SD and subsequent reperfusion failure (Figure 2(d)). The presence of P1 was seen more often in female mice (Figure 2(b)).

The bilateral presence of P1 was seen in 4 mice ($n=1/3$, male/female), in which only 2 SDs were detected. The unilateral absence of P1 in 12 mice ($n=9/4$, male/female) was invariably associated with the occurrence of SD in the ipsilateral hemisphere. In some of these mice ($n=4/1$, male/female), SD also occurred at the contralateral side in case the CBF in the contralateral cortex fell under the CBF threshold of SD initiation (Fig. S1). Finally, the bilateral absence of P1 in 9 mice ($n=4/5$, male/female) typically gave rise to SD in both hemispheres. The lower likelihood for SD to develop in female mice (Figure 1(c)) appeared to

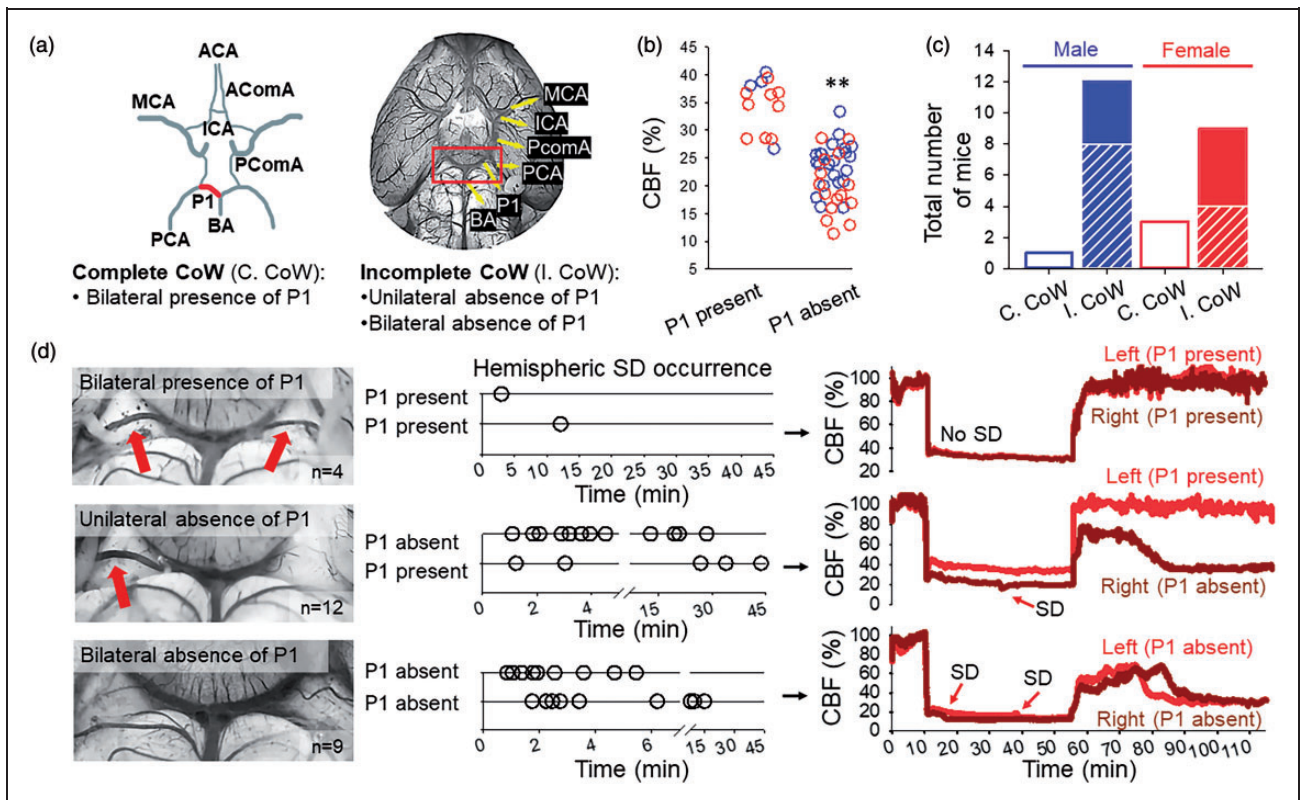


Figure 2. The absence of the P1 segment of the posterior cerebral artery (PCA) of the CoW predicts greater perfusion drop in response to CCA occlusion and subsequent SD occurrence. (a) The anatomy of the CoW (P1 segment in red) represented schematically along an original photomicrograph of the base of a mouse brain, vasculature filled with carbon ink. (b) CBF minimum measured shortly after ischemia induction in each hemisphere at the presence or absence of P1. Note that the absence of P1 is associated with lower CBF minimum (blue: male, red: female). (c) The prevalence of P1 anatomical variations in the CoW in male and female mice. Complete CoW (C.CoW) is shown as open bars, while incomplete CoW (I.CoW) is represented by dashed portions for the unilateral and closed portions for the bilateral absence of P1. (d) Selected photomicrographs demonstrate anatomical variations of the CoW. Red arrows show P1. Corresponding timelines indicate the temporal pattern of SDs detected in all our mice during 45 min ischemia. CBF traces depict representative reperfusion kinetics corresponding to the presence/absence of P1. Note that SDs under ischemia and reperfusion failure developed most frequently in the hemisphere ipsilateral to the absence of P1. ACA: anterior cerebral artery; AComA: anterior communicating artery; BA: basilar artery; ICA: internal carotid artery; MCA: middle cerebral artery; PComA: posterior communicating artery. The distribution of data (panel b) was evaluated with a Shapiro-Wilk test ($p = 0.483$), followed by a One-Way ANOVA with a Holm-Sidak post-hoc test, $p < 0.01^{**}$.

be linked to the higher incidence of a complete CoW (CoW: 4/12 vs. 1/13, female vs. male) (Figure 2(c)).

Neurological dysfunction and neuronal injury associated with reperfusion failure

Mice that suffered SD and reperfusion failure displayed considerable somatosensory neurological deficit as expressed on the GN scale a day after ischemia (14.5 ± 3.1 vs. 18.8 ± 0.8 , SD vs. no SD) (Figure 3(b)). Forelimb outstretching, lateral turning, and climbing were linked to SD occurrence and reperfusion failure (Figure 3(b₁)). In contrast, mice that experienced no SD and had adequate reperfusion performed close to their pre-ischemic, optimal function (18.8 ± 0.8 vs. 21.0 , post- vs. pre-ischemia) (Figure 3(b)). Further, higher composite GN score correlated closely with a higher level of reperfusion (Figure 3(c)). Finally, neuronal necrosis was more prominent ipsilateral to SD and reperfusion failure, in all brain regions analyzed (e.g. parietal cortex: 130 ± 2 vs. 97 ± 13 cell count/ $1000 \mu\text{m}^2$, SD vs. no SD) (Figure 3(d)).

Pharmacological SD inhibition to prevent reperfusion failure

NMDA receptor antagonists inhibit but not completely block SD.^{13,24} By the application of MK801, we set out to confirm that SD – rather than an incomplete CoW by itself – was implicated in reperfusion failure. As expected, MK801 curtailed SD, reflected by the smaller relative SD area (76.1 ± 10.4 vs. $87.7 \pm 6.5\%$, MK801 vs. vehicle) and the lower rate of SD propagation (3.2 ± 1.3 vs. 4.2 ± 1.4 mm/min, MK801 vs. vehicle) (Figure 4(a)). The smaller SD area in the MK801-treated group offered the opportunity to test the efficacy of reperfusion at a cortical region unaffected by SD in addition to the area covered by SD within the same hemisphere (Figure 4(b₁)). As shown earlier, reperfusion was impaired in the cortical area affected by SD; yet reperfusion was optimal in the same hemisphere in the area which had not been invaded by SD (78.8 ± 17.6 vs. $49.2 \pm 1.0\%$, SD non-affected area vs. SD affected area) (Figure 4(b₁₋₂)). In line with improving reperfusion via SD inhibition, the MK801-treated

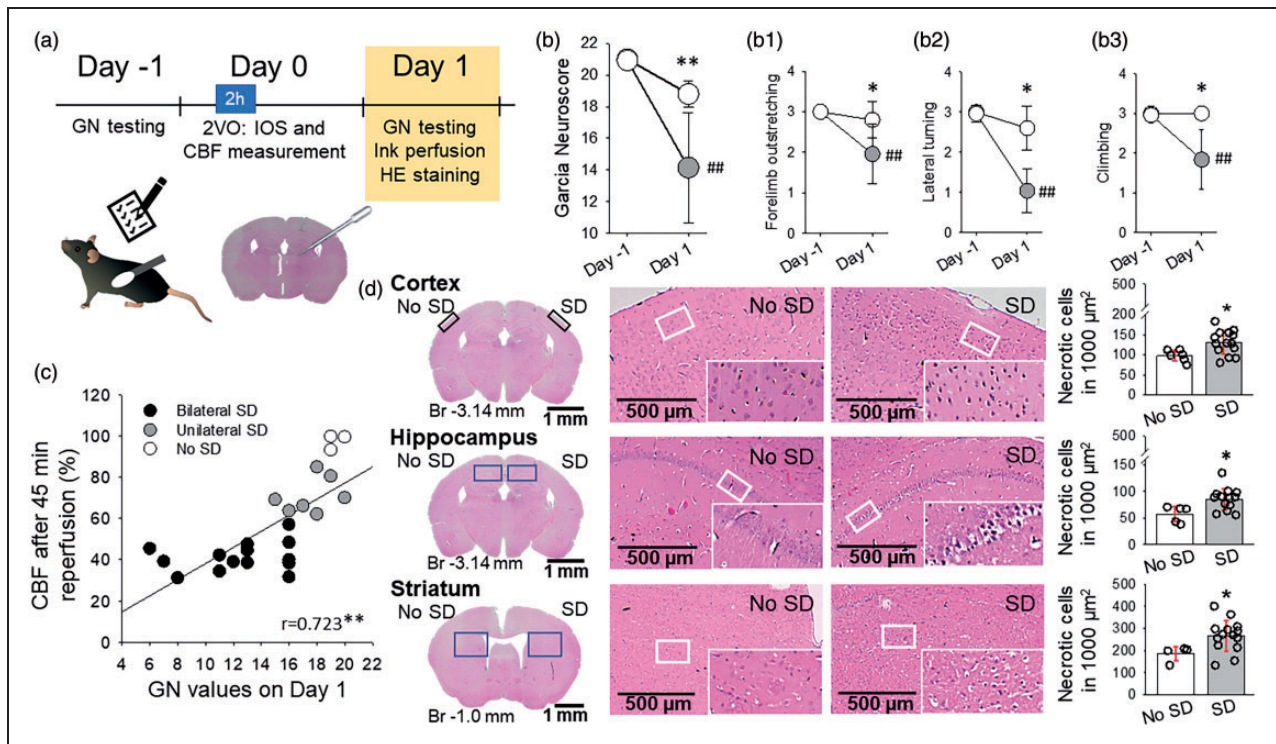


Figure 3. The occurrence of SD during ischemia and subsequent reperfusion failure are associated with severe neurological deficit and marked neuronal necrosis 24 h after ischemia. (a) The timeline of the experiments. (b) Neurological sensorimotor deficit expressed on the Garcia Neuroscore (GN) scale a day after ischemia, with respect to pre-ischemic performance. Selected motor test results revealed asymmetric motor function linked to SD occurrence. (c) Positive linear correlation between GN score and reperfusion failure taken 45 min into reperfusion. (d) Neuronal necrosis in hematoxylin-eosin (HE) stained sections. In b and d, data are given as mean \pm stdev. The distribution of data was evaluated by a Shapiro-Wilk test (b, $p = 0.599$, b₁, $p < 0.050$, b₂, $p < 0.050$, b₃, $p < 0.050$, C, $p = 0.281$, d, $p = 0.200$), followed by a One-Way RM ANOVA with Holm-Sidak post-hoc test (b), a Kruskal-Wallis ANOVA (b₁, b₂, b₃), a Two-Tailed Pearson correlation analysis (c) or one-way ANOVA with Holm-Sidak post-hoc test (d), $p < 0.05^*$ and $p < 0.01^{**}$ vs. No SD, $p < 0.01^{###}$ vs. Day-1.

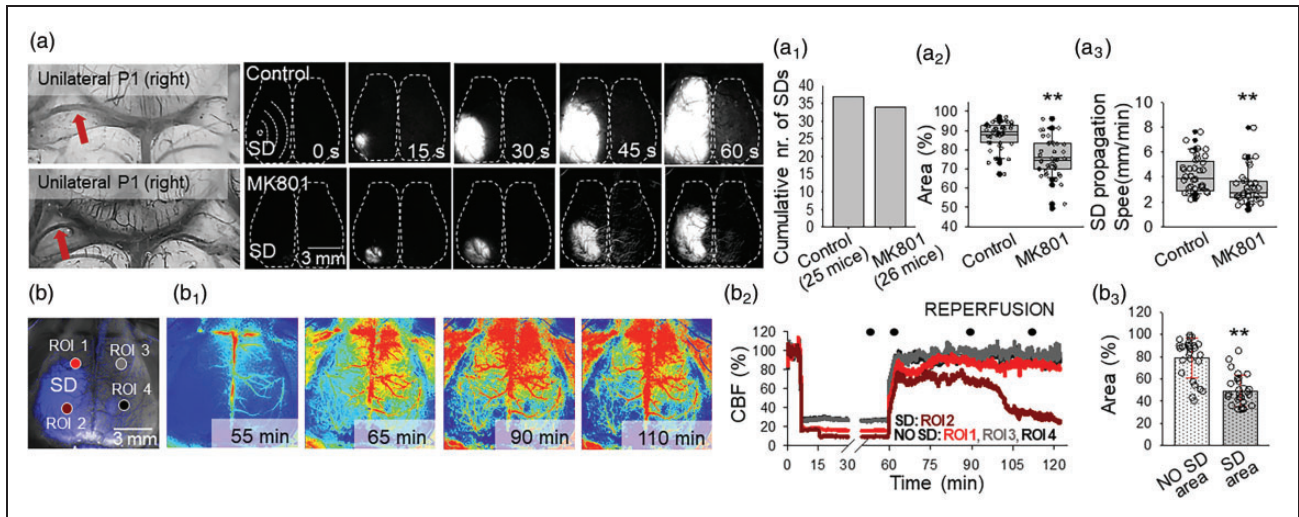


Figure 4. The pharmacological inhibition of SD counteracts reperfusion failure. (a) Representative images demonstrate the absence of the left PI at the base of the brain, and the corresponding evolution of SD in background subtracted IOS intensity images. Note that SD covered the entire ipsilateral cortex in a control mouse, while SD propagated a shorter distance in an MK801-treated preparation. MK801 did not block SD occurrence (a₁) but reduced the area of the cortical surface bearing SD (a₂) and decelerated SD propagation (a₃). (b) An IOS image demonstrates the cortical surface. In the left cortex, the area covered by SD is shown in blue. ROI1 was positioned over the surface unaffected by SD. In contrast, ROI2 was located within the area engaged in SD. ROI3-4 were placed over the contralateral cortex. The corresponding traces (b₁) and the quantitative analysis (b₂) reveal that reperfusion failure developed in the area previously engaged in SD (“SD area”), but reperfusion was sufficient in the same hemisphere in an area, which had not been reached by SD (“No SD area”). Data are given as mean±stdev. The distribution of data was evaluated by a Shapiro-Wilk test (a₂, $p = 0.123$, a₃, $p < 0.050$, b₃, $p = 0.050$), followed by a Mann-Whitney Rank Sum test (a₂ and a₃) or a T-test (D₃), $p < 0.05^*$, $p < 0.01^{**}$.

mice achieved higher score on the functional test a day after ischemia (GN score: 17.5 ± 1.9 vs. 14.6 ± 2.5 , MK801 vs. vehicle), although neuronal necrosis was not attenuated (Fig. S2).

Discussion

This is the first study to demonstrate the decisive role of SD in reperfusion failure following cerebral ischemia. Ischemic SD evolution emerges as a reliable predictor of inadequate reperfusion despite successful restoration of large vessel patency. This is a significant realization, because in almost half of stroke patients treated with endovascular therapy or thrombectomy, recanalization is futile, and functional outcome is poor despite optimal angiographic results.^{2,3}

Indeed, technically successful recanalization does not always ensure sufficient reperfusion or therapeutic benefit in ischemic stroke care.^{2,3} The unexpected inefficacy of reperfusion therapy is attributed in part to no-reflow. No-reflow manifests at the level of the microvascular network. Despite full recanalization of a large vessel, microcirculatory flow is not restored due to the compromised patency of small arterioles and capillaries.^{25,26} Interestingly, SD-related vasoconstriction has been recently shown to originate in the capillary bed in the mouse brain.²⁷ Further, even though the CBF response to SD commences within 30 s after SD,

subsequent oligemia in healthy brain tissue may last over an hour, and was found coincident with the impairment of cerebrovascular reactivity.^{28,29} Taken together, it is plausible that SD imposes decisive, persistent microvascular constriction and possibly capillary stall events, which reach beyond the ischemic period and are implicated in the later impairment of reperfusion.

The CBF response to SD is shaped by the actual balance between vasodilator and vasoconstrictor substances released in response to SD.²⁸ Under severe ischemia, vasoconstriction may override the response, which is known as spreading ischemia,³⁰ last as long as the depolarization itself, and has also been observed here (Figure 1(d₂)). The SD related vasoconstriction is governed by the high extracellular concentration of K^{+31} and accumulating arachidonic acid derivatives³² including 20-hydroxyecosatetraenoic acid (20-HETE)³³ and prostaglandin F₂ α (PGF₂ α).^{34,35} 20-HETE and PGF₂ α appear to mediate the long lasting oligemia after SD in optimally perfused tissue.³³⁻³⁵ Moreover, 20-HETE was shown to impair vasodilation evoked by neuronal activation in experimental focal cerebral ischemia,³⁶ which may be analogous with the depression of dilation to SD in ischemic brain tissue.^{37,38} Taken together, we suggest that early reperfusion failure linked to SD here is possibly mediated by the

accumulation of vasoconstrictive substances long-lasting in the wake of SD and sustained into the early phase of reperfusion. We are currently exploring this possibility experimentally in detail.

Another significant observation of this study is that SD occurrence was associated with a critically low CBF related to reduced collaterals of the CoW. Anatomical anomalies of the CoW are common in the C57BL/6J mouse strain²², as well as in the healthy adult human population.³⁹ The absence or hypoplasia of the P1 segment of the PCA, the second most frequent vascular attenuation in human CoW anomalies³⁹ caused in our mice a significantly greater drop of CBF after CCA occlusion. The drop of CBF below a critical level was followed by SD occurrence, which corresponds with the concept of a hypoperfusion threshold of SD generation.³⁸ In fact, low collateral grade in stroke patients correlates with larger final infarct volumes and worse long-term neurologic deficit.⁴⁰

Pharmacological SD inhibition in our model prevented reperfusion failure despite the absence of the P1 segment of the PCA, substantiating the link between SD occurrence and insufficient reperfusion further. NMDA receptor antagonism with MK801 limited SD propagation but did not block SD occurrence entirely, and improved neurological function without restraining necrotic cell death. The partial benefits of NMDA receptor antagonism may be attributed to the ligand binding properties of the receptor. For example, high extracellular K^+ levels typical of the developing ischemic infarct appear to reduce the efficacy of MK801.²⁴ Tissue acidosis considerable in the ischemic core was also shown to inhibit Ca^{2+} influx through NMDA receptors,⁴¹ impeding any further benefit expected of pharmacological NMDA receptor antagonism. Potassium ion and pH gradients in the ischemic brain tissue, therefore, may modulate the efficacy of NMDA receptor blockade.

Both male and female mice were used in this study without expecting sexual dimorphism in the readouts.⁴² At close inspection of the data, we have found a lower incidence of SD in female mice. The lower SD frequency corresponded to a higher incidence of a complete CoW predicting a smaller CBF drop after vascular occlusion in female mice. Therefore, the better collateral circulation itself appeared to account for the fewer SDs – rather than any potential sex-related factor concerning ischemic tolerance or SD susceptibility.

The incomplete global forebrain ischemia (2VO) model used may be perceived as a limitation. A considerable advantage of the 2VO model is that a uniform penumbra-like condition is created in the entire forebrain in contrast with the thin and barely reproducible penumbra layer in rodent focal ischemia models. Most importantly, the 2VO model served best our purposes

here because SD may or may not occur after bilateral carotid occlusion, dependent on the magnitude of the post-occlusion perfusion drop (Figure 1(e)). This condition enabled the assessment of the effects of SD superimposed on ischemic penumbra-like conditions.

In conclusion, we put forward the novel concept that SD is a main contributor to reperfusion failure despite successful recanalization after stroke. The novel conceptual aspect of the work is that reperfusion failure – which was previously linked to several mechanisms including microthrombosis, distal capillary constriction by pericytes, capillary stalls with neutrophils, large vessel constriction, and distal clot embolization^{4,26} – is a consequence of SD that occurs during ischemia. Moreover, our findings suggest that poor collaterals lead to a more severe drop of blood flow after cerebrovascular occlusion, which creates favorable conditions for SD initiation. Collateral rarefaction and insufficiency accompany cerebral aging and worsen stroke outcomes with aging.^{43,44} This may increase the relevance of our findings taken that stroke incidence increases exponentially in the aging population. Next, we propose that the underlying mechanism of reperfusion failure due to SD is sustained vasoconstriction, which may manifest primarily at the level of the microvascular bed. Finally, the reperfusion failure after SD appears to predict aggravated neurological deficit and poor outcomes after stroke. Understanding the cause of futile recanalization and identifying SD as an underlying factor may guide new therapeutic options to improve stroke outcomes.

Funding

The author(s) disclosed receipt of the following financial support for the research, authorship, and/or publication of this article: the EU's Horizon 2020 research and innovation program under grant agreement No. 739593; grants from the National Research, Development and Innovation Office of Hungary (No. K134377 and K134334); the Ministry of Innovation and Technology of Hungary and the National Research, Development and Innovation Fund (No. TKP2021-EGA-28 financed under the TKP2021-EGA funding scheme); the Ministry of Human Capacities of Hungary (ÚNKP-21-3-SZTE-78) and the National Brain Research Program 3.0 of the Hungarian Academy of Sciences.

Declaration of conflicting interests

The author(s) declared no potential conflicts of interest with respect to the research, authorship, and/or publication of this article.

Authors' contributions

ÁM and EF designed the study; AT, RT, and ÁM conducted experiments; AT, RT, SDB, SS and ÁM acquired data; AT, RT, SDB, SS and ÁM analyzed data; FB and EF supervised

the work and provided funding; AT, ÁM and EF wrote the manuscript.

ORCID iD

Eszter Farkas  <https://orcid.org/0000-0002-8478-9664>

Supplemental material

Supplemental material for this article is available online.

References

- Rha JH and Saver JL. The impact of recanalization on ischemic stroke outcome: a meta-analysis. *Stroke* 2007; 38: 967–973.
- Hussein HM, Georgiadis AL, Vazquez G, et al. Occurrence and predictors of futile recanalization following endovascular treatment among patients with acute ischemic stroke: a multicenter study. *AJNR Am J Neuroradiol* 2010; 31: 454–458.
- Espinosa de Rueda M, Parrilla G, Manzano-Fernandez S, et al. Combined multimodal computed tomography score correlates with futile recanalization after thrombectomy in patients with acute stroke. *Stroke* 2015; 46: 2517–2522.
- Amki ME and Wegener S. Reperfusion failure despite recanalization in stroke: new translational evidence. *Clin Transl Neurosci* 2021; 5: 2514183X2110071.
- Woitzik J, Hecht N, Pinczolits A, et al. Propagation of cortical spreading depolarization in the human cortex after malignant stroke. *Neurology* 2013; 80: 1095–1102.
- Dohmen C, Sakowitz OW, Fabricius M, et al. Spreading depolarizations occur in human ischemic stroke with high incidence. *Ann Neurol* 2008; 63: 720–728.
- Pinczolits A, Zdunczyk A, Dengler NF, et al. Standard-sampling microdialysis and spreading depolarizations in patients with malignant hemispheric stroke. *J Cereb Blood Flow Metab* 2017; 37: 1896–1905.
- Sueiras M, Thonon V, Santamarina E, et al. Cortical spreading depression phenomena are frequent in ischemic and traumatic penumbra: a prospective study in patients with traumatic brain injury and large hemispheric ischemic stroke. *J Clin Neurophysiol* 2021; 38: 47–55.
- Menyhart A, Frank R, Farkas AE, et al. Malignant astrocyte swelling and impaired glutamate clearance drive the expansion of injurious spreading depolarization foci. *J Cereb Blood Flow Metab* 2022; 42: 584–599.
- Somjen GG. Mechanisms of spreading depression and hypoxic spreading depression-like depolarization. *Physiol Rev* 2001; 81: 1065–1096.
- Dreier JP, Lemale CL, Kola V, et al. Spreading depolarization is not an epiphenomenon but the principal mechanism of the cytotoxic edema in various gray matter structures of the brain during stroke. *Neuropharmacology* 2018; 134: 189–207.
- Toth OM, Menyhart A, Varga VE, et al. Chitosan nanoparticles release nimodipine in response to tissue acidosis to attenuate spreading depolarization evoked during forebrain ischemia. *Neuropharmacology* 2020; 162: 107850.
- Andrew RD, Farkas E, Hartings JA, et al. Questioning glutamate excitotoxicity in acute brain damage: the importance of spreading depolarization. *Neurocrit Care* 2022; 37: 11–30.
- Gerkau NJ, Rakers C, Durry S, et al. Reverse NCX attenuates cellular sodium loading in metabolically compromised cortex. *Cereb Cortex* 2018; 28: 4264–4280.
- Reinhart KM and Shuttleworth CW. Ketamine reduces deleterious consequences of spreading depolarizations. *Exp Neurol* 2018; 305: 121–128.
- Hartings JA, Andaluz N, Bullock MR, et al. Prognostic value of spreading depolarizations in patients with severe traumatic brain injury. *JAMA Neurol* 2020; 77: 489–499.
- Dreier JP, Winkler MKL, Major S, et al. Spreading depolarizations in ischaemia after subarachnoid haemorrhage, a diagnostic phase III study. *Brain* 2022; 145: 1264–1284.
- Luckl J, Lemale CL, Kola V, et al. The negative ultrasound potential, electrophysiological correlate of infarction in the human cortex. *Brain* 2018; 141: 1734–1752.
- Hartings JA, Shuttleworth CW, Kirov SA, et al. The continuum of spreading depolarizations in acute cortical lesion development: examining Leao's legacy. *J Cereb Blood Flow Metab* 2017; 37: 1571–1594.
- Farkas E, Bari F and Obrenovitch TP. Multi-modal imaging of anoxic depolarization and hemodynamic changes induced by cardiac arrest in the rat cerebral cortex. *Neuroimage* 2010; 51: 734–742.
- Krafft PR, McBride DW, Lekic T, et al. Correlation between subacute sensorimotor deficits and brain edema in two mouse models of intracerebral hemorrhage. *Behav Brain Res* 2014; 264: 151–160.
- Fujii M, Hara H, Meng W, et al. Strain-related differences in susceptibility to transient forebrain ischemia in SV-129 and C57black/6 mice. *Stroke* 1997; 28: 1805–1810; discussion 1811.
- Hecht N, He J, Kremenetskaia I, et al. Cerebral hemodynamic reserve and vascular remodeling in C57/BL6 mice are influenced by age. *Stroke* 2012; 43: 3052–3062.
- Petzold GC, Windmuller O, Haack S, et al. Increased extracellular K⁺ concentration reduces the efficacy of N-methyl-D-aspartate receptor antagonists to block spreading depression-like depolarizations and spreading ischemia. *Stroke* 2005; 36: 1270–1277.
- Soares BP, Chien JD and Wintermark M. MR and CT monitoring of recanalization, reperfusion, and penumbra salvage: everything that recanalizes does not necessarily reperfuse! *Stroke* 2009; 40: S24–27.
- El Amki M and Wegener S. Improving Cerebral blood flow after arterial recanalization: a novel therapeutic strategy in stroke. *Int J Mol Sci* 2017; 18: 2669.
- Anzabi M, Li B, Wang H, et al. Optical coherence tomography of arteriolar diameter and capillary perfusion during spreading depolarizations. *J Cereb Blood Flow Metab* 2021; 41: 2256–2263.
- Ayata C and Lauritzen M. Spreading depression, spreading depolarizations, and the cerebral vasculature. *Physiol Rev* 2015; 95: 953–993.
- Lacombe P, Sercombe R, Correze JL, et al. Spreading depression induces prolonged reduction of cortical

- blood flow reactivity in the rat. *Exp Neurol* 1992; 117: 278–286.
30. Dreier JP. The role of spreading depression, spreading depolarization and spreading ischemia in neurological disease. *Nat Med* 2011; 17: 439–447.
 31. Menyhart A, Farkas AE, Varga DP, et al. Large-conductance Ca(2+)-activated potassium channels are potentially involved in the inverse neurovascular response to spreading depolarization. *Neurobiol Dis* 2018; 119: 41–52.
 32. Shibata M, Leffler CW and Busija DW. Prostanoids attenuate pial arteriolar dilation induced by cortical spreading depression in rabbits. *Am J Physiol* 1991; 261: R828–834.
 33. Fordsmann JC, Ko RW, Choi HB, et al. Increased 20-HETE synthesis explains reduced cerebral blood flow but not impaired neurovascular coupling after cortical spreading depression in rat cerebral cortex. *J Neurosci* 2013; 33: 2562–2570.
 34. Gariépy H, Zhao J and Levy D. Differential contribution of COX-1 and COX-2 derived prostanoids to cortical spreading depression-evoked cerebral oligemia. *J Cereb Blood Flow Metab* 2017; 37: 1060–1068.
 35. Varga DP, Szabo I, Varga VE, et al. The antagonism of prostaglandin FP receptors inhibits the evolution of spreading depolarization in an experimental model of global forebrain ischemia. *Neurobiol Dis* 2020; 137: 104780.
 36. Li Z, McConnell HL, Stackhouse TL, et al. Increased 20-HETE signaling suppresses capillary neurovascular coupling after ischemic stroke in regions beyond the infarct. *Front Cell Neurosci* 2021; 15: 762843.
 37. Hertelendy P, Menyhart A, Makra P, et al. Advancing age and ischemia elevate the electric threshold to elicit spreading depolarization in the cerebral cortex of young adult rats. *J Cereb Blood Flow Metab* 2017; 37: 1763–1775.
 38. Menyhart A, Zolei-Szenasi D, Puskas T, et al. Spreading depolarization remarkably exacerbates ischemia-induced tissue acidosis in the young and aged rat brain. *Sci Rep* 2017; 7: 1154.
 39. Iqbal S. A comprehensive study of the anatomical variations of the circle of Willis in adult human brains. *J Clin Diagn Res* 2013; 7: 2423–2427.
 40. Kimmel ER, Al Kasab S, Harvey JB, et al. Absence of collaterals is associated with larger infarct volume and worse outcome in patients with large vessel occlusion and mild symptoms. *J Stroke Cerebrovasc Dis* 2019; 28: 1987–1992.
 41. Plutino S, Sciacaluga M and Fucile S. Extracellular mild acidosis decreases the Ca(2+) permeability of the human NMDA receptors. *Cell Calcium* 2019; 80: 63–70.
 42. Harriott AM, Chung DY, Uner A, et al. Optogenetic spreading depression elicits trigeminal pain and anxiety behavior. *Ann Neurol* 2021; 89: 99–110.
 43. Riddle DR, Sonntag WE and Lichtenwalner RJ. Microvascular plasticity in aging. *Ageing Res Rev* 2003; 2: 149–168.
 44. Faber JE, Zhang H, Lassance-Soares RM, et al. Aging causes collateral rarefaction and increased severity of ischemic injury in multiple tissues. *Arterioscler Thromb Vasc Biol* 2011; 31: 1748–1756.